Hindawi
Geofluids
Volume 2021, Article ID 8858030, 13 pages
https://doi.org/10.1155/2021/8858030

Research Article

Investigation on the Influence of Temperature and Confining Pressure on the Hydraulic Conductivity of the Integrated and Fractured Jurassic Conglomerates

Dingyang Zhang,[1,2] **Wanghua Sui**,[1] **and Jiawei Liu**[1]

[1]*School of Resources and Geosciences, State Key Laboratory for Geomechanics and Deep Underground Engineering, China University of Mining and Technology, 1 Daxue Rd., Xuzhou, Jiangsu 221116, China*
[2]*School of Geology and Geomatics, Tianjin Chengjian University, 26 Jinjing Rd., Tianjin 300380, China*

Correspondence should be addressed to Wanghua Sui; suiwanghua@cumt.edu.cn

Received 11 July 2020; Accepted 31 May 2021; Published 22 June 2021

Academic Editor: Ilaria Fuoco

This paper presents an experimental investigation on the properties of hydraulic conductivity and permeability of conglomerates under different temperatures and confining pressures with integrated samples and samples with shear failure. Constant head tests were carried out in a temperature-controlled triaxial cell with samples obtained from the Zhuxianzhuang Coal Mine. Five levels of temperatures (10°C, 20°C, 28°C, 35°C, and 50°C) and three levels of confining pressures (3 MPa, 5 MPa, and 7 MPa) were chosen for the tests. The results show that there is a negative relationship between hydraulic conductivity and confining pressure with both original and shear failure samples. An inflection point of 35°C is found in the relationship between the flow rate and temperature. However, with increasing temperature conditions, hydraulic conductivity first increases and then decreases at 50°C with the intact sample, while hydraulic conductivity first decreases from 20°C and then increases with the shear failure sample. Finally, nonlinear regression equations of hydraulic conductivity and temperature were obtained under different confining pressures.

1. Introduction

Multiple fields, such as temperature, stress, and seepage, are coupling around rock masses. Therefore, based on existing theory and practice, an investigation of the characteristics of permeability in both an integrated and a fractured rock mass under the combined interactions of seepage, stress, and temperature is necessary for understanding the stability of rock slopes and underground surroundings. Understanding the permeability of a fractured rock mass is one of the fundamental issues in the study of fluid flow in fractured rock masses. Temperature and pressure vary with the depth of strata and geological conditions. Due to geothermal gradients, within a certain depth, temperature increases with depth, while in different stratigraphic structures, the surrounding pressure also changes. In different stratigraphic structures, the confining pressure and the ambient temperature of the rock mass are different, which affects the permeability characteristics, and these factors cannot be ignored.

Many researchers have studied the flow in an integrated rock mass, and the characteristics of the flow are relatively simple and regular [1–3]. The hydraulic conductivity of porous media is a fundamental property that determines the durability of these media and the flow rate through them. The permeability of a fractured rock mass is crucial to influencing water flow through the internal cavities underground. Some researchers have carried out in situ hydraulic tests [4, 5], physical model tests [6], and numerical analysis [7] of the characteristics of flow in fractured rock mass. Lomize [8] first began to measure the flow in fractured rock by establishing a parallel-plate model, which was later used in grouting theory and experiments [9]. The impact of variable confining pressure on the seepage properties of fractured rocks was investigated under different confining pressures by

Ma et al. [10] through experiments and theory. Miao et al. [11] established a hollow cylinder apparatus to study the non-Darcy flow and to measure water flow in rock blocks in deformation-restricted conditions. Huang et al. [3] presented an in situ high-pressure fluid injection experimental investigation of hydraulic properties of deep natural fractured rocks, providing valuable insight for evaluating the evolution of that of the surrounding rocks in relation to water inrush.

In recent years, studies have paid attention to the coupled thermo-hydro-mechanical-chemical(THMC) effect on underground engineering constructions [12]. The coupled THM processes have been modelled using a number of different methods [13]. Nishimura et al. [14] developed a formulation of the coupled THM finite element code to study freeze and thaw in water-saturated soils. Na and Sun [15] presented a finite strain formulation for frozen porous media to investigate the freeze-thaw action of frozen porous media by applying multiplicative kinematics. Yasuhara et al. [16] developed a coupled THMC model for examining the long-term change in the permeability of porous sedimentary rocks, predicting the expected stress and temperature conditions.

Temperature varies with the depth of strata, and the inclusion of thermal effects into hydraulic properties becomes increasingly prevalent [17]. Ye et al. [18] investigated the effects of temperature on the hydraulic conductivity of bentonite samples. The hydraulic conductivity of bentonite shows a positive correlation with temperature (20°C, 40°C, 50°C, and 60°C), but the changing paths of temperature (cooling or heating) have no effect on the hydraulic conductivity. In our conglomerate sample case, the relationships of hydraulic conductivity with temperatures of 10°C, 20°C, 28°C, 35°C, and 50°C show a nonlinear variation. Ma et al. [19] presented an experimental study investigating the anisotropic properties of the hydraulic conductivity of Boom clay and the corresponding influence of the heating-cooling cycle. The results show that the hydraulic conductivity is not sensitive to the heating rate, but there is a positive relationship between the hydraulic conductivity and temperatures of 23°C, 40°C, 60°C, and 80°C. Ahlem Houaria et al. [20] compared the water and gas permeabilities of concretes after cooling from different temperatures (200°C, 300°C, 400°C, 600°C, and 700°C). They found that the permeability increased with temperature but decreased at temperatures of 400°C and 600°C. Piscopo et al. [21] proposed a relationship between hydraulic conductivity and rock mass depth, which showed an exponentially declining trend with depth. An exponential relationship was found between the hydraulic conductivity and temperature of sandstone at the temperature between 20°C and 800°C according to Xu and Yang [22]. However, laboratory studies on the influences of temperature and confining pressure on the hydraulic conductivity of both integrated and fractured conglomerates are limited.

Experimental investigations have shown that temperature has a great influence on the strength, deformation, damage, and healing characteristics of rock mass [23, 24]. Gao et al. [25] found that mechanical strength was improved under liquid nitrogen cooling conditions and that the average fracture toughness of the rock was greater than that of the original rocks. The creation and propagation of microcracks were promoted with cooling conditions [26, 27]. Li et al. [28] investigated the mechanical characteristics influenced by the temperature of surrounding rocks and found that the ultimate tensile force, which is dependent on temperature, obeyed a cubic polynomial function. The effect of temperature on the breakage energy, yield force, breakage force, and elasticity modulus of individual particles was also investigated [29]. Nassr et al. [30] modelled the effects of confining pressure and temperature on frozen soils.

In this study, an attempt was made to study the hydraulic conductivity of conglomerates in the laboratory under various thermal-hydro-mechanical conditions. For this purpose, an experimental study was conducted using constant head tests. Samples were extracted from the overburden layers of the Jurassic System in the Zhuxianzhuang Coal Mine in Anhui Province, China. The layers were then reinforced by grouting to decrease the hydraulic connection of the neighboured aquifers. The test confining pressure ranged from 3 MPa to 7 MPa, including its in situ confining pressure. Five levels of temperature, 10°C, 20°C, 28°C, 35°C, and 50°C, were tested, and these temperatures correspond to the environmental temperatures at particular depths from 0 m to 1000 m underground. Thus, the present work puts a new contribution to the understanding of the different factors that control the hydraulic conductivity of conglomerates, particularly those related to variable geological environments. These factors may have an important contribution in future studies of predicting the hydraulic conductivity properties of the grouting area. For example, it may be important to consider these influences in the study of grouted conglomerates or the sealing efficiency of grouted conglomerates related to variable geological environments.

2. Materials and Method

2.1. Samples and Their Geological Background. The study area is located in the Zhuxianzhuang Coal Mine in Anhui Province, China, as shown in Figure 1. The stratigraphic succession of the study area contains sequences from the Ordovician, Carboniferous, Permian, Jurassic, Neogene, and Quaternary Systems. The stratigraphic column is shown in Figure 2.

The main studied stratum is the Jurassic System. It is a set of fuchsia continental sediments, with a maximum exposed thickness of 240 m. The lower part is a conglomerate section with a thickness of 0~100 m and an average thickness of 50~60 m. The main components of the gravel are limestone with a small amount of sandstone and metamorphic rocks. The cementation is mainly calcareous cement, followed by muddy and sandy matrix. The conglomerate and the underlying coal measures are unconformable, and the denudation dip is 15~25°. The middle part is interbedded with siltstone, sandstone, and conglomerate, with obvious multilayered coarse and fine sedimentary rhythms. The upper siltstone has a fine grain size, has clear layering, and contains argillaceous inclusions. The bedding plane tends to the northeast, and the dip angle is 10~20°. The thicknesses of the middle and upper layers are approximately 106 m. Influenced by bedrock morphology control and late denudation, the upper Jurassic strata are preserved in the low-lying area, with

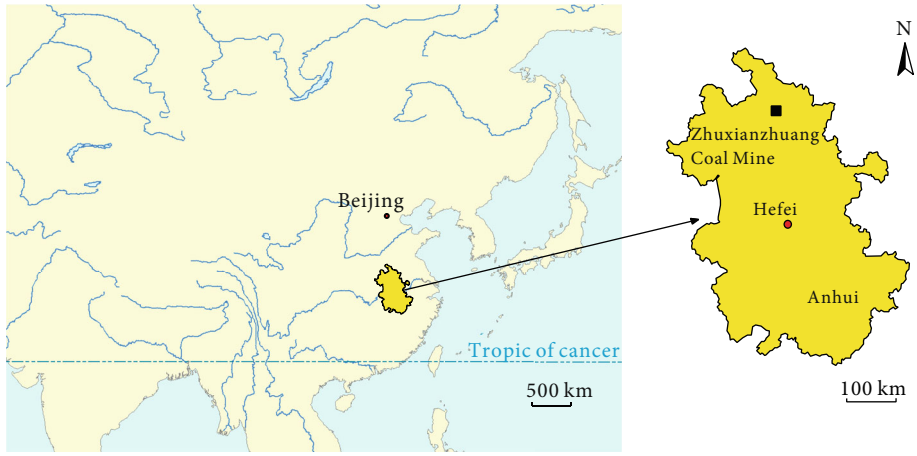

Figure 1: Location of the Zhuxianzhuang Coal Mine.

shaping like a long tongue from north to south, which enters the northeast corner of the mine. It contains the fifth aquifer of the study area.

The fifth aquifer is in unconformable contact with the fourth aquifer and the coal seams, which is a result of sedimentation of the mountain floodplain. The gravel components are mostly limestone from limestone fragments, with a gravel diameter of 0.2~7 cm and poor sorting. The cementation is purple-red clay materials. The thickness is controlled by the ancient topography of the area, which is thicker in shallow and western parts and gradually thins and pinches toward the deep and eastern areas. The erosion surface is roughly parallel with the coal seam, tending to the northeast. The thickness is 44~102 m, with a dip angle of 15~25°. The water richness of the fifth aquifer is determined by the degree of karst development. As karst development is very uneven, the specific capacity of water from the different sections varies from 0.29 to 4.38 L/s·m. The water richness increases with the thickness of the conglomerate layers from south to north. The fifth aquifer has a strong connection with the Ordovician limestone aquifer, which is why the fifth aquifer is hard to be dewatered or depressured. This is why a grout curtain is built at the interface of these two aquifers: to cut off the connection.

Conglomerate samples, extracted at depths of 300-400 m from the study area, are used to carry out permeability tests. The samples are composed mainly of purple conglomerates and sandstone. Conglomerates are a kind of sedimentary clastic rock composed of quartzite, limestone, and other heterogeneous rocks. Argillaceous, calcareous, and ferric materials cement them. The dominant fraction of this kind of conglomerate contains limestone and clay. Karst caves are well developed. The fifth aquifer threatens the safety of underground engineering, which supports the investigation of the hydraulic conductivity of the conglomerates in the event of an emergency.

2.2. Experimental Setup and Procedures. A temperature-controlled triaxial testing machine with a hyperbaric environment in Global Digital Systems (GDS) carried out the constant head tests. The device contains a conventional triaxial apparatus with a pressure chamber, pore water pressure measurement system with different kinds of sensors, and a temperature controller and data logger (Figure 3). An oil pressure generator supplies the confining pressure, while the back water pressure and the base water pressure are applied by two hydraulic pressure generators. The heater coil is set up inside the chamber wall and is powered by the temperature controller with simethicone circulation. A temperature sensor is placed inside the chamber in the cell fluid. The maximum temperature is 60°C with an accuracy of 0.1°C. The maximum confining pressure is 64 MPa, and the maximum vertical loading is 400 kN.

The sample is fixed on the base of the main pressure chamber with permeable stone placed up and down. On the top of the sample is a cap with a hole reserved for connecting water from the back pressure controller to the pore water within samples. A pressure chamber covers the sample, sealing off water and air. Simethicone is injected into the pressure chamber and acts as the transfer medium for the confining pressure. The confining pressure controller regulates the release or the increase in the confining pressure, along with measuring and recording the results. The temperature module also uses simethicone as a medium for temperature increase and decrease, which is achieved by the oil inlet in the oil-bath machine. The seepage module uses water as the seepage medium. The top and bottom of the sample distribute both water injection and drainage holes, respectively. The injection hole is connected to the back pressure controller to monitor the water seepage rate. The bottom is connected to the base pressure controller and a pore water pressure transducer for measuring the pore water pressure and changes in pore water volume, respectively. The triaxial shearing module elevates the base of the sample at a constant rate to make the top of the sample contact with the control element for shearing process. All data in each test module are collected by the GDSLAB computer system.

Cylindrical samples with standard diameters (50 mm) and heights (100 mm) were used in the test. The sample saturation and vacuuming procedure was performed to avoid air presence before the test started. The uniaxial compressive strength was applied in consideration of the end effect.

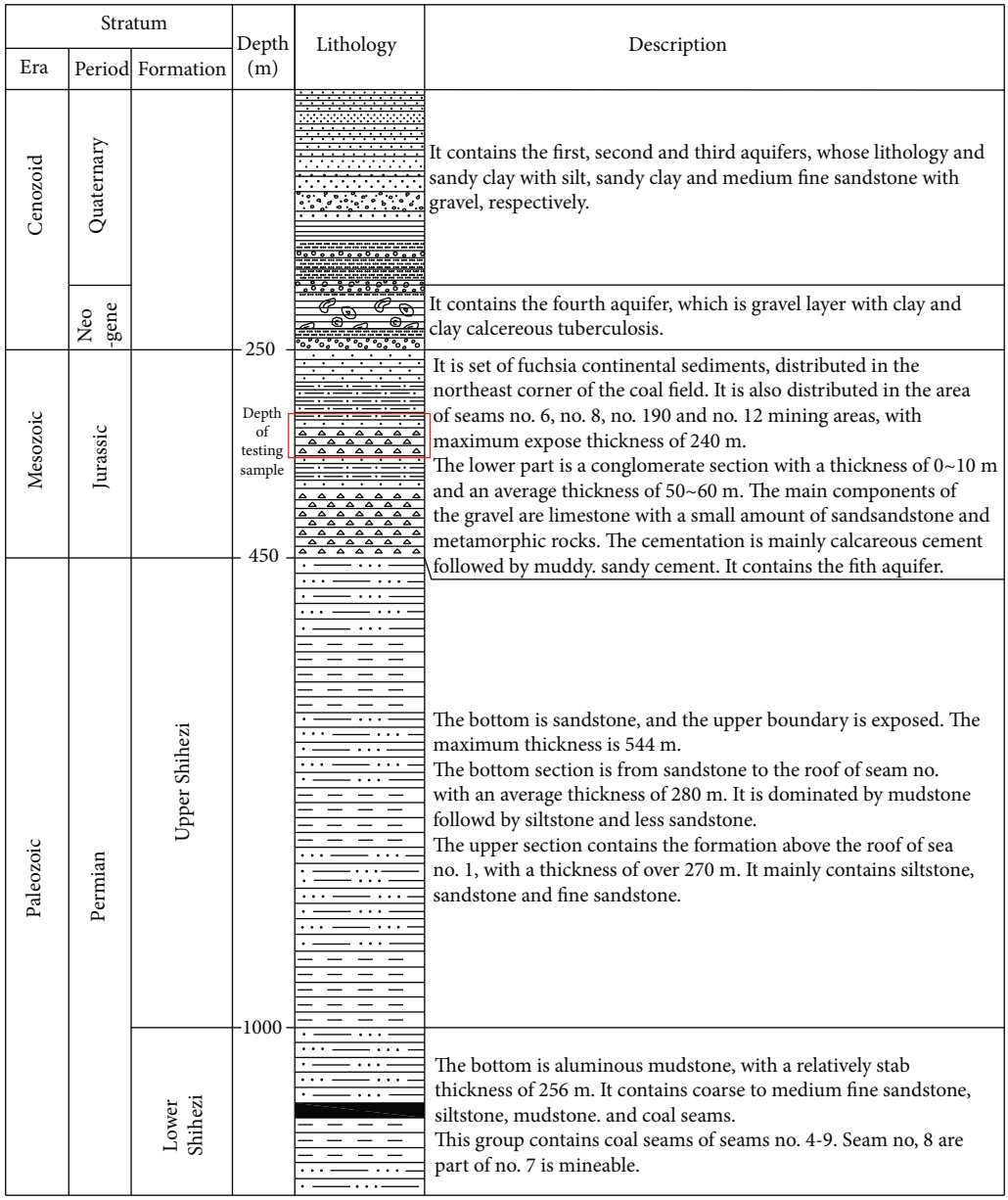

Figure 2: The stratigraphic column of the study area.

Limestone breccia rock blocks were extracted from a depth approximately 350 m underground. The samples were prepared from the limestone breccia rock blocks by the following procedure. Firstly, the samples (cylindrical cores) were prepared parallel to the bedding plane of the studied stratigraphic column. Then, the samples were saturated fully in deionized water in a water-submergible vacuum jar, in order to eliminate the air in the pores and cracks. The test confining pressures are chosen as 3 MPa, 5 MPa, and 7 MPa, and 3 MPa was the closest in situ pressure of this study area. Temperature varies with the formation depth and geological conditions. Within a certain depth, temperature increases with increasing depth, and the main transitive method is heat conduction. The normal average earth thermal gradient below the constant temperature layeris that the temperature rises by 3°C for every 100 m deeper. The temperature changes discussed in this article are mainly concentrated in the range of 1000 m below the surface. It is because most underground constructions including tunnels, subway, and coal mines are conducted within this range. Since the rock blocks were extracted at the depth of 300-400 m from the study area, and the surrounding temperature is around 35°C, this level was selected. In order to compare with other temperature conditions of other situation, the levels of temperature are chosen as 10°C, 20°C, 28°C (room temperature), 35°C, and 50°C.

The test procedures are as follows:

(1) Sample loading. A saturated sample was removed, and excess water was wiped with filter paper. Heat

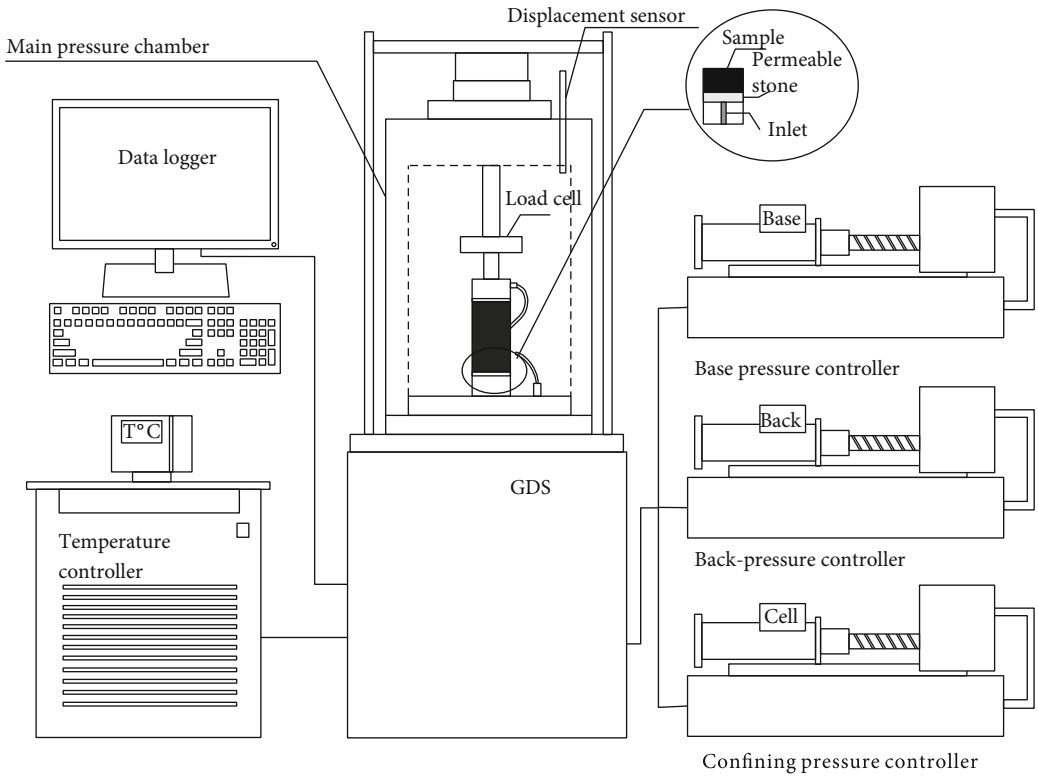

Figure 3: Hyperbaric environment of Global Digital Systems (GDS).

(a) (b) (c)

Figure 4: (a) Heat shrink tape, (b) warm air machine, and (c) rock sample.

shrink paper that is 7 cm longer than the length of the rock sample was placed outside the sample (Figure 4(a)). By using a warm air machine, the paper was shrunk to fit the surface of the rock sample (Figure 4(b)). Two metal permeable stones were placed on both ends of the specimen, which was then placed on the base of the main pressure chamber. The upper part was capped with a sample cap and shrink paper. The contact portion of the paper with the base and the sample cap is tightly heat-shrunk together to eliminate all air. A titanium oxide loop tightly covers both ends to prevent oil and water from entering and mixing (Figure 4(c)). Figure 5 shows a detailed schematic diagram of sealing the test sample. The three-piece fastener is then tightened. When using the temperature module, an insulation cover should be added outside the pressure chamber. Figure 6 shows how the heating function works

(2) Cleared. All controllers are cleared in air, and the axial force is cleared after loading

(3) Controller debug. Clear the label volume to zero for each controller

(4) Test the tightness. Connect all sensors and controllers and use an oil pump to inject oil into the pressure chamber. The computer controls the confining pressure of 200 kPa and tests whether there are any leaks from the instruments

(5) Conduct the test. Create a new test within the GDSLAB system software. Select the module for permeability-temperature and select the data file. Enter the sample size and other detailed information.

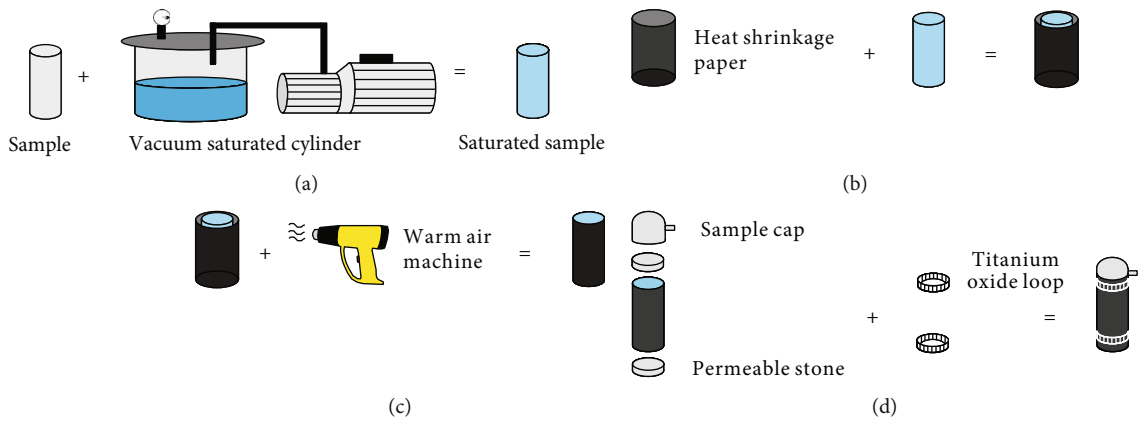

Figure 5: Schematic diagram of sealing the test sample.

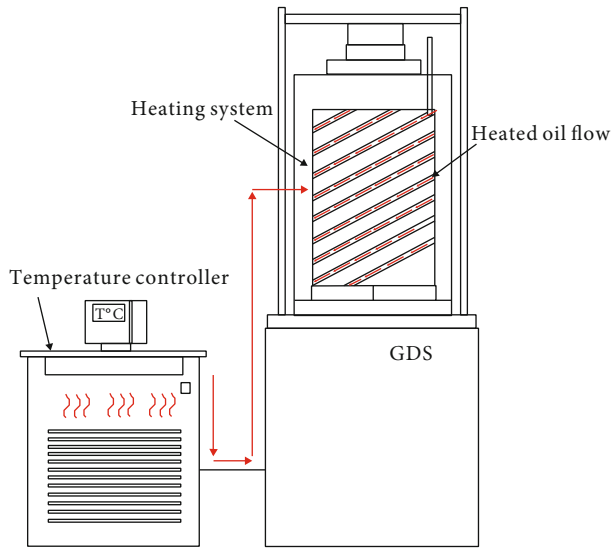

Figure 6: Heating process.

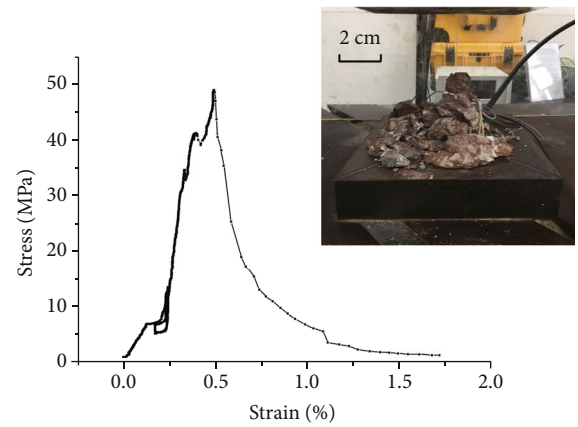

Figure 7: Stress-strain curves and the shape after crushing of conglomerate sample.

Then, select new sample; add a test phase, such as a permeability test; and set the confining pressure, back pressure, and pressure difference. The pressure difference remains the same in this test

(6) Save the test. Output data and pictures

3. Results and Analysis

3.1. The UCS of the Dry and Saturated Samples. Considering the effect of the end effect, uniaxial compressive strength (UCS) was conducted for the mechanical properties of the rock sample. The WES-D1000 electrohydraulic servo tester was used for testing. The UCSs of the conglomerates under dry and saturated conditions are 43.3 MPa and 31.1 MPa, respectively. The peak value of the saturated sample was first reached, and the UCS of the saturated condition was less than that of the dry condition. Figure 7 shows the stress strain relationship under dry conditions.

3.2. Effects of Temperature on the Hydraulic Conductivity of the Original Samples. The temperature sensibility of simethicone, which is used as both a cell fluid and heating fluid, was tested by observing the variation in oil volume (cell volume) with changing temperature (see Figure 8).

When heating the cell fluid, the temperature increased by stage, from 10°C to 20°C, then from 20°C to 28°C, until it reached 50°C. In the cooling process, the temperature decreased from 50°C to 10°C directly. The results show that during both temperature processes, the cell volume and the temperature form anapproximately linear dependence relationship. During the stage process, the increasing rate was fast at first, but the rate went more slowly as the target temperature was approached.

Figure 9 shows the seepage flow under various temperature levels with the original samples when the confining pressures are 3 MPa, 5 MPa, and 7 MPa.

When the confining pressure was 3 MPa, the flow rate was 14.86 mL/min at 10°C and increased to 23.93 mL/min at 35°C but decreased to 2.57 mL/min at 50°C. The same result was observed for the confining pressure of 7 MPa; the flow rate increased from 0.93 mL/min at 10°C to 3.75 mL/min at 35°C and then decreased to 1.17 mL/min at 50°C. At 5 MPa, the flow rate decreased from 28°C with a value of 12.08 mL/min, which is different from the conditions of 3 MPa and 7 MPa. The rate at 10°C was 2.42 mL/min, and at

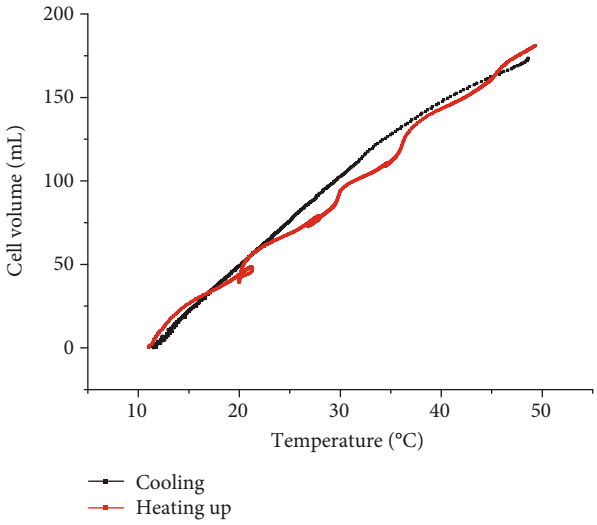

Figure 8: Cell volume changes with temperature.

50°C, the rate was 2.16 mL/min. Three same-condition samples were conducted in this test, and the changing tendency of 50°C is different from the other four conditions for each test. The results show that with increasing temperature, the flow rate increases in each confining pressure condition. Under the condition of 50°C, the confining pressure has less effect on the flow rate than the other temperature conditions. During the seepage progression, both the seepage fluid and samples were influenced in response to changing temperatures.

3.3. Effects of Temperature on the Hydraulic Conductivity of the Samples with Shear Failure. After the completion of the permeability test of the complete conglomerate sample, a triaxial standard compression/shear test was carried out on the same sample under the confining pressure of 7 MPa, which produced cracks. The maximum axial stress of shear failure was 241.11 kN, and the maximum deformation failure occurred at a strain of 1.27%.

Figure 10 shows the seepage flow under various temperatures with the shear failure samples when the confining pressure was 3 MPa, 5 MPa, and 7 MPa.

After generating fissures, the permeability of the sample obviously increased. Regardless of the confining pressure, the steady seepage flow rate increased with increasing temperature. At 3 MPa, the seepage flux increased from 452.09 mL/min at 10°C to 530.10 mL/min at 50°C. The seepage flux increased from 288.59 mL/min at 10°C to 320.44 mL/min at 50°C when the confining pressure was 5 MPa. At 7 MPa, the seepage flux increased from 166.43 mL/min at 10°C to 371.23 mL/min at 50°C. With shear failure cracks, a large seepage passageway formed in the test rock mass. The maximum seepage fluxes at each confining pressure stage are 22.15 times, 26.53 times, and 98.99 times greater than those of the original samples. The viscosity of water was the dominant factor influencing the flow rate during the heating process. As the temperature increased, the viscosity decreased, and the flow rate increased [31–33].

3.4. Effects of Confining Pressure on the Hydraulic Conductivity of Both Samples. The hydraulic conductivity shows an obvious decreasing trend with increasing confining pressure. The decreasing amplitude of the seepage flow was different at various temperatures. Before the temperature reached 50°C, the variation range of the permeate flux increased from 3 MPa to 5 MPa, but the range was relatively small from 5 MPa to 7 MPa. However, the decreased magnitude of the seepage flow was similar to these two stages at 28°C. When the temperature reached 50°C, the variation in the flow rate at these three confining pressure stages was small. However, it still showed a reduction trend with increasing confining pressure.

The same variation trend occurred for samples with shear failure cracks. The seepage flow rate decreased gradually with increasing confining pressure, except when the temperature reached 50°C. The steady flow rates were similar at 5 MPa and 7 MPa, and those at 7 MPa were higher. Except for 50°C, the variation range of the seepage flow at each confining pressure stage was almost the same.

4. Discussion

4.1. Differences in the Influence of Confining Pressure and Temperature on Integrated and Fractured Rock Samples. The environment of the fractured rock mass mainly includes three aspects: seepage field (groundwater), stress field, and thermal field (geothermal). In this geological environment, a change in the environment causes fracture rock changes in the structural and mechanical effects on the rock mass. The water pressure generated by the change in the seepage water level in the crack or discontinuity initiates the change in the pore water pressure. According to the principle of effective stress, the effective stress decrease between the particles reduces the normal stress of the surrounding rock. At the same time, the seepage could physically weaken the rock mass, thereby changing the stress field. However, the change in the stress field leads to structural changes in cracks or discontinuities, which include changes in crack openings, connectivity, and porosity, and then changes the permeability of cracks and discontinuous structures; this is the coupling of the seepage field and stress field. The seepage fluid acts as a medium for propagating thermal energy, performing thermal convection, and performing heat conduction in the fracture medium and the discontinuous surface. Then, the heat generated by the change in temperature changes the density, viscosity, and flow rate of the fluid, which shows the coupling of the seepage field and the thermal field. The change in stress causes structural changes in the fractures and discontinuities, resulting in energy conversion, which changes the thermodynamic parameters of the rock mass structure or water flow, such as thermal conductivity. This results in changes in thermal conductivity and temperature field redistribution. The change in temperature field changes the physical properties of cracks or discontinuities in the rock mass structure, such as thermal expansion and contraction. It may also generate thermal stress and thermal strain. The coupling of the stress field and the thermal field acts similar to this. The thermal-hydro-mechanical coupling is a dynamic

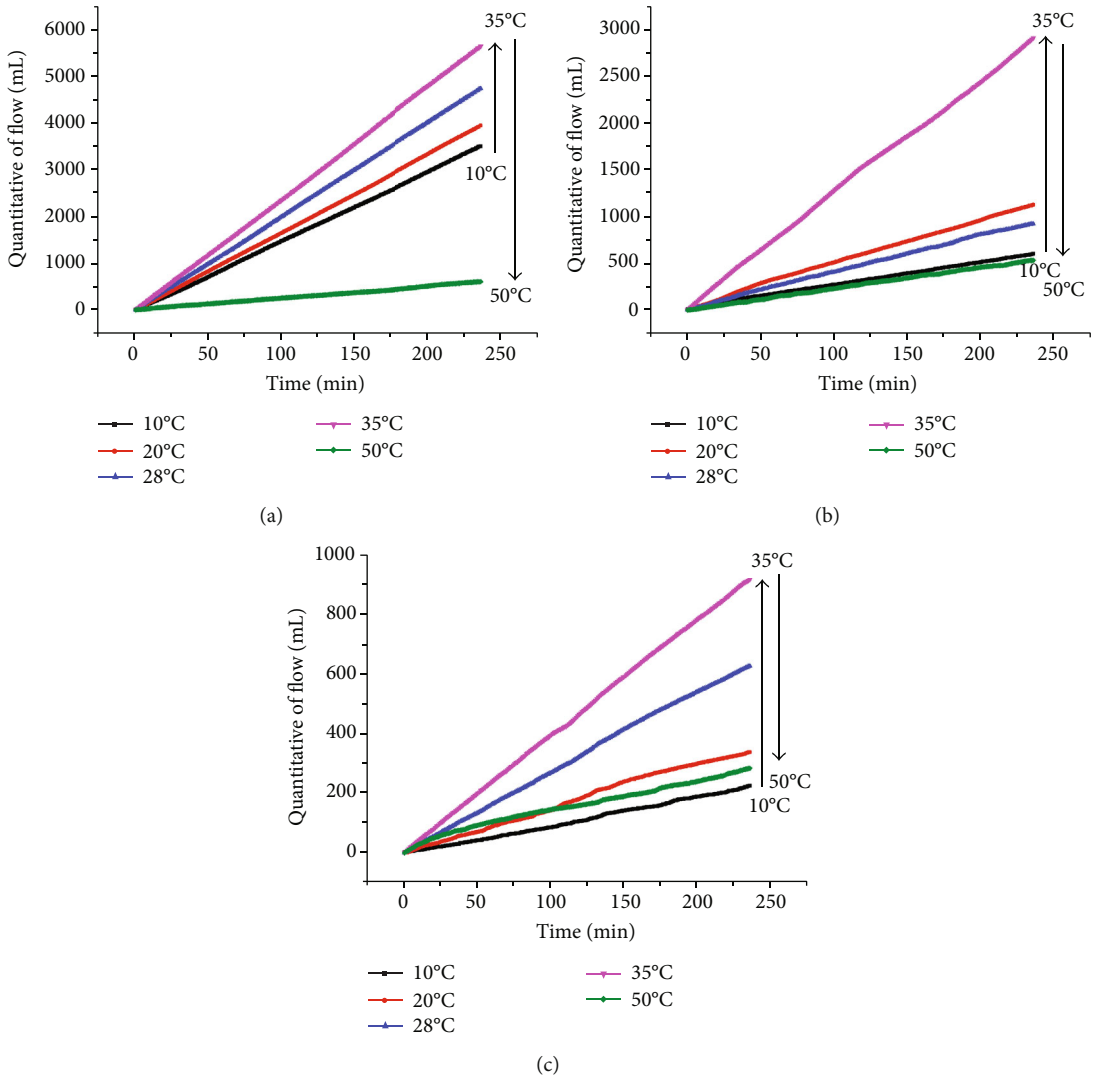

Figure 9: Seepage flow rate changes in the original samples with various temperatures when the confining pressures are (a) 3 MPa, (b) 5 MPa, and (c) 7 MPa.

process that constitutes a cyclical action chain; that is, the change in one field inevitably causes another field to change, and the change in the other field in turn affects the change in the previous field. This is a loop that constantly repeats until it reaches dynamic equilibrium.

Under the same confining pressure condition, the stable flow rate in each temperature section of the original conglomerate sample increases with increasing temperature. The maximum value occurs at 35°C. The steady seepage at each temperature section of fractured samples increases with temperature. Under the same temperature conditions, the permeate flux of the original and fractured samples decreases with increasing confining pressure. During the seepage progression in the integrated samples, both the seepage fluid and samples were influenced in response to changing temperatures. The general changes are that the viscosity of water decreases with the heating process and that the rock mass expands with heating and contracts with cooling. However, the testing results show that the seepage flow rate does not correspond directly with the heating process. At low temperatures, the viscosity of water is dominated by temperature. As the viscosity of water decreases, the velocity of water increases, and the seepage flux increases. When the temperature reaches a certain value, the thermal expansion and contraction of the rock sample volume dominate the temperature effect. During the heating process, the rock mass expands, which compacts the cracks and pores inside the sample. This is equivalent to reducing the seepage area of the cross-flow section, which results in reduced seepage flow.

The variation in the seepage flow of fractured conglomerates with confining pressure is similar to that of intact conglomerates. The seepage flow gradually decreases with increasing confining pressure. The fracture caused by shearing forms a steady flow inside the rock sample. The influence of the pressure change on the pore structure of entire sample is much smaller than that of the shear fracture. During the increase in pressure, there was a compacted environmental condition on the rock sample, which changed the structure of the cracks and pores in the rock sample. Then, the connectivity decreased. At the same time, as the confining pressure

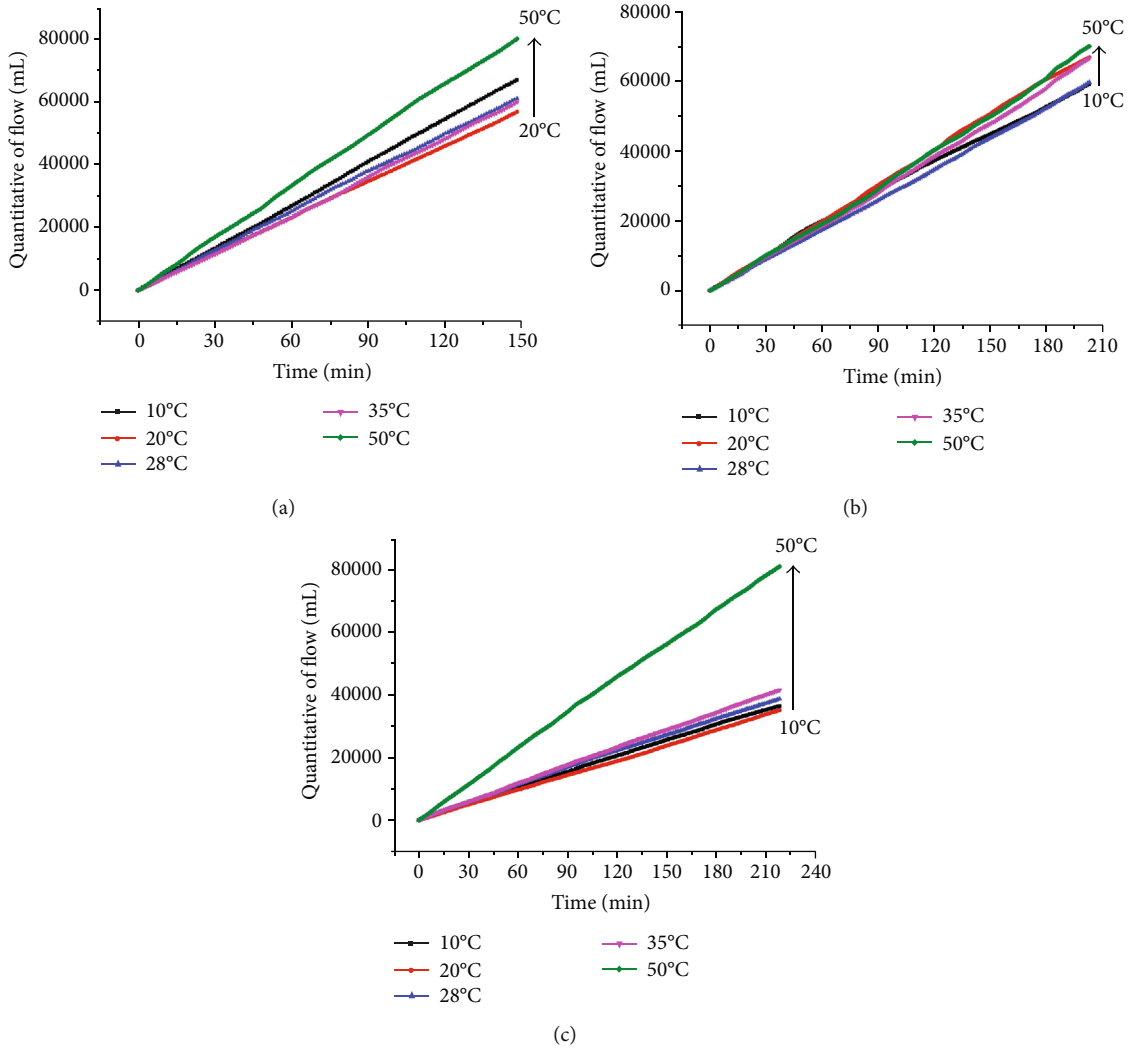

FIGURE 10: Seepage flow rate changes in the shear failure samples with various temperatures when the confining pressures are (a) 3 MPa, (b) 5 MPa, and (c) 7 MPa.

increased, the state of liquid molecules became closer. The molecular motion was hindered, which increased the viscosity of the liquid. However, there was little change in viscosity with pressure when groundwater was in the general geostress environment, which basically occurs under conditions less than 60 MPa.

4.2. Analysis of the Impact on Hydraulic Conductivity. The conglomerates were subjected to laboratory tests on the hydraulic conductivity of integrated and fractured samples under different temperatures and confining pressures. According to Darcy's law and the standard of triaxial permeability test from the Operation Manual of GDSLAB2.5, Equation (1) was used to calculate the testing results.

$$k = \frac{q \bullet L}{A \bullet \Delta h}, \tag{1}$$

where q is the specific discharge (m^3/s), L is the length of the seepage path (m), A is the flow section (m^2), and Δh is the head difference (m).

The hydraulic gradient was calculated by the equation of $I = \Delta h/L$, where $\Delta h = 50$ m, and $L = 0.1$ m. So, the hydraulic gradient is 500. The seepage pressure difference is $\Delta P = 1$ MPa, and the flow section is $A = 0.0019625\ m^2$. The results are shown in Figure 11 and Table 1. F-tests were performed by using different functions for correlation analysis. P values were less than 0.1 for the cubic and quadratic polynomial. The optimum nonlinear regression equations between temperature and hydraulic conductivity were achieved under different confining pressures, as shown in Table 2.

According to the quantitative relationships above, it can be concluded that in general, the relationships between the hydraulic conductivity and temperature conditions of integrated and fractured samples are affected by Equations (2) and (3), respectively.

$$K = aT^3 + bT^2 + cT + d, \tag{2}$$

$$K = aT^2 + bT + c, \tag{3}$$

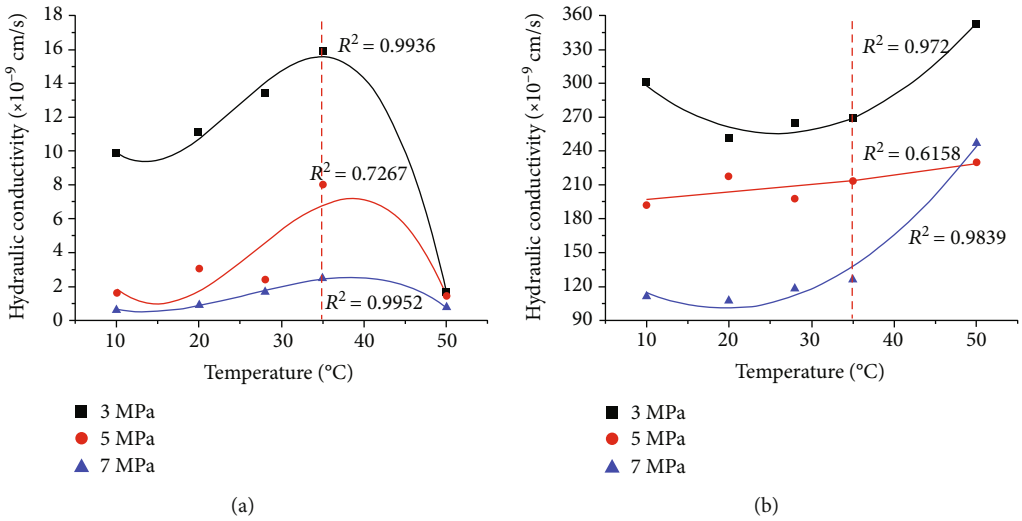

Figure 11: Relationships among hydraulic conductivity, permeability, and temperature for the integrated (a) and fractured (b) samples.

where a, b, c, and d are the coefficients related to the confining pressures.

For the integrated rock samples, the coefficients of the polynomial are linearly related to the confining pressures, that is, $a = a_1P + b_1$. Then, Equation (4) is obtained.

$$K = (a_1P + b_1)T^3 + (a_2P + b_2)T^2 + (a_3P + b_3)T + a_4P + b_4, \tag{4}$$

where a_1, b_1, etc. are constants.

Porosity is three-dimensional, and T^3 presents the effect of temperature on the pores and fluids. The expansion or contraction of volume is three-dimensional. Permeability and viscosity are a two-dimensional concept, and T^2 presents the influence of temperature on the permeability and the viscosity. T presents a constant value of surrounding temperature, which matches the confining pressure, P. The regression formula shows that when the temperature and confining pressure change, the water conductivity varies due to the expansion and contraction of pores and the changes in permeability and viscosity.

The hydraulic conductivity gradually increases below 35°C, reaching its peak at 35°C, then decreases at 50°C. At temperatures below 35°C, hydraulic conductivity reaches what is called the gradually increase phase. The change in temperature results in changes in fluid viscosity, which is the main reason for the increase in hydraulic conductivity. At temperatures higher than 35°C, the volume of pores decreases with the expansion of the rock part and then decreases. This phase is called the sudden decrease phase.

When the fractured sample is at temperatures <35°C, the hydraulic conductivity increases at a low speed, or it might fluctuate. This phase is called the stagnant phase. At temperatures >35°C, the hydraulic conductivity increases at a high speed, and this is called the quick increase phase. Compared with other references, Alam et al. [34] performed the hydraulic conductivity test under the temperature conditions of 295 K (21.85°C) and 393 K (119.85°C) and different confining pressure ranges from 1 to 15 MPa. The permeabilities of the granite with confining pressures of 3 MPa, 5 MPa, and 7 MPa were 2×10^{-6} μm^2, 3×10^{-6} μm^2, and 9.4×10^{-6} μm^2 for 21.85°C and 9.3×10^{-6} μm^2, 2.4×10^{-6} μm^2, and 9.8×10^{-7} μm^2 for 119.85°C, respectively. And the permeabilities of the sandstone were 1×10^{-6} μm^2, 4.9×10^{-5} μm^2, and 7.9×10^{-5} μm^2 for 21.85°C, and 6.2×10^{-5} μm^2, 9×10^{-5} μm^2, and 1×10^{-6} μm^2 for 119.85°C, respectively. The influence of temperature and confining pressure also fluctuated. Zhang et al. [35] conducted the experiments under the temperature conditions of 25°C, 50°C, and 100°C and confining pressure conditions of 0.6 MPa, 1.0 MPa, and 1.4 MPa for fine sandstone. Results show that the permeability first increased and then decreased in 0.6 MPa, and kept decreasing in 1.0 MPa, and first decreased and then increased in 1.4 MPa, respectively.

In addition, since the molecular structure of the solid matter is relatively tight with respect to the liquid molecules, within a certain temperature range, the temperature has little effect on the physical and mechanical indexes of the rock sample. Therefore, it can be considered that the effect of lower temperature on the fractured rock mass is small. Thus, the volume of fracture decreases slightly compared to that of the pore holes. In other words, temperature has less influence on large holes or fractures, which causes the different developing trends observed for the hydraulic conductivity of integrated and fractured samples.

The permeability of fractured rock mass is one of the fundamental issues in the problem of fluid flow in engineering projects. Temperature and confining pressure vary with the depth of strata and geological conditions. Here, it presents the temperature variables to distinguish different depths of the project locations. In different stratigraphic structures, the confining pressure and the ambient temperature of the rock mass are different, as are the permeability characteristics. By using this analysis, it could predict the permeability features for the potential safety problems of underground projects.

Table 1: Hydraulic conductivity of conglomerate samples.

State	Pressure difference (ΔP (MPa))	Confining pressure (P (MPa))	Temperature (T (°C))	Hydraulic conductivity (K ($\times 10^{-9}$cm/s))	Permeability (k ($\times 10^{-5}\mu m^2$))
Integrated	1	3	10	9.88	1.32
			20	11.13	1.14
			28	13.38	1.15
			35	15.91	1.18
			50	1.71	0.10
		5	10	1.61	0.21
			20	3.08	0.32
			28	2.42	0.21
			35	8.03	0.60
			50	1.43	0.08
		7	10	0.62	0.08
			20	0.91	0.09
			28	1.70	0.15
			35	2.49	0.18
			50	0.78	0.04
Fractured	1	3	10	300.61	40.13
			20	251.12	25.80
			28	264.74	22.67
			35	268.55	19.92
			50	352.47	20.00
		5	10	191.89	25.61
			20	217.58	22.35
			28	197.64	16.92
			35	213.07	15.80
			50	230.02	13.05
		7	10	110.66	14.77
			20	106.91	10.98
			28	117.93	10.10
			35	126.47	9.38
			50	246.84	14.00

Table 2: Nonlinear regression curve equation.

State of sample	Confining pressure (MPa)	Analytical expression	R^2
Integrated	3	$y = -0.0013x^3 + 0.0929x^2 - 1.1845x + 20.098$	0.9936
	5	$y = -0.0009x^3 + 0.0741x^2 - 1.5902x + 11.291$	0.7267
	7	$y = -0.0003x^3 + 0.0204x^2 - 0.4052x + 2.9047$	0.9952
Fractured	3	$y = 0.1674x^2 - 8.6472x + 367.14$	0.972
	5	$y = 0.0075x^2 + 0.3384x + 192.86$	0.6158
	7	$y = 0.1536x^2 - 5.975x + 158.77$	0.9839

4.3. Application for Grouting Projects. The hydraulic conductivity of conglomerate changes with different temperatures and confining pressures, which correspond to conglomerate layers located at different depths of the strata. To better understand the water flow in the conglomerate layers, the experiments present a more precise result of the real environment of rock masses. Conglomerate samples obtained from the study area correspond to the conditions of 35°C and 3 MPa. The results under other conditions provide an experimental basis for conglomerate layers in different strata,

which correspond to different environmental temperatures and confining pressures. The relationships among rock mass permeability, temperature, and confining pressure can be useful in engineering projects when the projects are conducted at different depths and in different geologic environments.

This paper presents the first step in investigating the study area in which grouting treatment is needed. The results could reflect the permeability characteristics of the strata where there are porous spaces between aquifers in the study area. By determining the permeability characteristics, the grouting distribution is predicted to achieve the relationships among the grouting diameter, grouting amount, and grouting pressure. Then, the grouting diameter and grouting amount used in the project are calculated. The permeability of the grouted samples under different conditions of temperature and confining pressure will be investigated in the future. By combining the limitations, it can find the effectiveness of grouting treatment in preventing water inrush in underground projects, which will also provide an experimental and theoretical basis for grouting engineering treatment.

5. Conclusions

The influence of confining pressure and temperature on the permeability of a fractured rock mass was studied. Based on the geological environment of the Jurassic strata in the study area, different confining pressures (3 MPa, 5 MPa, and 7 MPa) and temperatures (10°C, 20°C, 28°C, 35°C, and 50°C) were selected, and permeability tests were performed on the in situ collected rock samples using the GDS high-pressure environmental triaxial tester. The results are as follows:

(1) At the same confining pressure, a stable flow rate in each temperature section of the integrated conglomerate sample increases with increasing temperature. Two phases were proposed. At temperatures below 35°C, it is called the gradually increase phase. While at temperatures higher than 35°C, the phase is called the sudden decrease phase

(2) The interior of the rock sample formed a large hydraulic pathway after a triaxial shear test, resulting in a dramatic increase in percolation flow compared to that of the integrated rock sample. At this time, the viscosity of water mainly dominated the hydraulic conductivity. As the temperature increases, the viscosity decreases, the flow rate increases, and the seepage flow increases

(3) The seepage flow notably decreases with increasing confining pressure, but the decreasing range shows different performances at different temperatures. At the condition of 50°C, the change in seepage flow rate from 3 MPa to 5 MPa is larger, and the change range from 5 MPa to 7 MPa is relatively small

(4) The variation in seepage flow in fractured conglomerates with confining pressure is similar to that in intact conglomerates. The seepage flow gradually decreases with increasing confining pressure. The fracture caused by shearing forms a steady flow inside the rock sample. The influence of the pressure change on the pore structure at the intact part with the sample is much smaller than that of the shear fracture

Data Availability

The authors confirm that the data supporting the findings of this study are available within the article and are available from the corresponding author on request.

Conflicts of Interest

The authors declare that they have no conflicts of interest.

Acknowledgments

The authors would like to acknowledge the financial support of the National Key R&D Program under Grant No. 2017YFC1501303 and the National Natural Science Foundation of China Grant No. 41902292. The help on experiments for this paper from Longhan Zhang, Shichong Yuan, and Cong Xie from the China University of Mining and Technology is greatly appreciated.

References

[1] M. A. Biot, "General theory of three-dimensional consolidation," *Journal of Applied Physics*, vol. 12, no. 2, pp. 155–164, 1941.

[2] F. Thauvin and K. K. Mohanty, "Network modeling of non-Darcy flow through porous media," *Transport in Porous Media*, vol. 31, no. 1, pp. 19–37, 1998.

[3] Z. Huang, X. Z. Li, S. J. Li, K. Zhao, and R. Zhang, "Investigation of the hydraulic properties of deep fractured rocks around underground excavations using high-pressure injection tests," *Engineering Geology*, vol. 245, pp. 180–191, 2018.

[4] Y. F. Chen, M. M. Liu, S. H. Hu, and C. B. Zhou, "Non-Darcy's law-based analytical models for data interpretation of high-pressure packer tests in fractured rocks," *Engineering Geology*, vol. 199, pp. 91–106, 2015.

[5] Z. Huang, Z. Q. Jiang, X. Tang, X. S. Wu, D. C. Guo, and Z. C. Yue, "In situ measurement of hydraulic properties of the fractured zone of coal mines," *Rock Mechanics and Rock Engineering*, vol. 49, no. 2, pp. 603–609, 2016.

[6] D. Ma, M. Rezania, H. S. Yu, and H. B. Bai, "Variations of hydraulic properties of granular sandstones during water inrush: effect of small particle migration," *Engineering Geology*, vol. 217, pp. 61–70, 2017.

[7] O. Kresse, X. Weng, H. Gu, and R. Wu, "Numerical modeling of hydraulic fractures interaction in complex naturally fractured formations," *Rock Mechanics and Rock Engineering*, vol. 46, no. 3, pp. 555–568, 2013.

[8] G. M. Lomize, *Flow in fractured rocks [Ph.D. thesis]*, University of Gosemergoizdat, 1951.

[9] W. H. Sui, J. Y. Liu, W. Hu, J. F. Qi, and K. Y. Zhan, "Experimental investigation on sealing efficiency of chemical grouting in rock fracture with flowing water," *Tunnelling and Underground Space Technology*, vol. 50, pp. 239–249, 2015.

[10] D. Ma, X. X. Miao, Z. Q. Chen, and X. B. Mao, "Experimental investigation of seepage properties of fractured rocks under different confining pressures," *Rock Mechanics and Rock Engineering*, vol. 46, no. 5, pp. 1135–1144, 2013.

[11] X. X. Miao, W. Q. Liu, and Z. Q. Chen, *Seepage Theory of Mining Strata*, Science Press, Beijing, 2004.

[12] W. Ruhaak, V. F. Bense, and I. Sass, "3D hydro-mechanically coupled groundwater flow modelling of Pleistocene glaciation effects," *Computers & Geosciences*, vol. 67, pp. 89–99, 2014.

[13] S. Kelkar, K. Lewis, S. Karra et al., "A simulator for modeling coupled thermo-hydro-mechanical processes in subsurface geological media," *International Journal of Rock Mechanics and Mining Sciences*, vol. 70, pp. 569–580, 2014.

[14] S. Nishimura, A. Gens, S. Olivella, and R. Jardine, "THM-coupled finite element analysis of frozen soil: formulation and application," *Geotechnique*, vol. 59, no. 3, pp. 159–171, 2009.

[15] S. H. Na and W. C. Sun, "Computational thermo-hydro-mechanics for multiphase freezing and thawing porous media in the finite deformation range," *Computer Methods in Applied Mechanics and Engineering*, vol. 318, pp. 667–700, 2017.

[16] H. Yasuhara, N. Kinoshita, S. Ogata, D. S. Cheon, and K. Kishida, "Coupled thermo-hydro-mechanical-chemical modeling by incorporating pressure solution for estimating the evolution of rock permeability," *International Journal of Rock Mechanics and Mining Sciences*, vol. 86, pp. 104–114, 2016.

[17] G. J. Chen, T. Maes, F. Vandervoort et al., "Thermal impact on damaged Boom clay and Opalinus clay: permeameter and isostatic tests with μCT scanning," *Rock Mechanics and Rock Engineering*, vol. 47, no. 1, pp. 87–99, 2014.

[18] W. M. Ye, M. Wan, B. Chen, Y. G. Chen, Y. J. Cui, and J. Wang, "Temperature effects on the swelling pressure and saturated hydraulic conductivity of the compacted GMZ01 bentonite," *Environment and Earth Science*, vol. 68, no. 1, pp. 281–288, 2013.

[19] Y. S. Ma, W. Z. Chen, H. D. Yu, Z. Gong, and X. L. Li, "Variation of the hydraulic conductivity of Boom clay under various thermal-hydro-mechanical conditions," *Engineering Geology*, vol. 212, pp. 35–43, 2016.

[20] M. B. Ahlem Houaria, M. Abdelkader, C. Marta, and K. Abdelhafid, "Comparison between the permeability water and gas permeability of the concretes under the effect of temperature," *Energy Procedia*, vol. 139, pp. 725–730, 2017.

[21] V. Piscopo, A. Baiocchi, F. Lotti et al., "Estimation of rock mass permeability using variation in hydraulic conductivity with depth: experiences in hard rocks of western Turkey," *Bulletin of Engineering Geology and the Environment*, vol. 77, no. 4, pp. 1663–1671, 2018.

[22] P. Xu and S. Q. Yang, "Influence of stress and high-temperature treatment on the permeability evolution behavior of sandstone," *Acta Mechanica Sinica*, vol. 35, no. 2, pp. 419–432, 2019.

[23] W. G. P. Kumari, P. G. Ranjith, M. S. A. Perera, B. K. Chen, and I. M. Abdulagatov, "Temperature-dependent mechanical behaviour of Australian Strathbogie granite with different cooling treatments," *Engineering Geology*, vol. 229, pp. 31–44, 2017.

[24] W. J. Li, C. Zhu, C. H. Yang, K. Duan, and W. R. Hu, "Experimental and DEM investigations of temperature effect on pure and interbedded rock salt," *Journal of Natural Gas Science and Engineering*, vol. 56, pp. 29–41, 2018.

[25] F. Gao, C. Z. Cai, and Y. G. Yang, "Experimental research on rock fracture failure characteristics under liquid nitrogen cooling conditions," *Results in Physics*, vol. 9, pp. 252–262, 2018.

[26] M. Cha, X. Yin, T. Kneafsey et al., "Cryogenic fracturing for reservoir stimulation - laboratory studies," *Journal of Petroleum Science and Engineering*, vol. 124, pp. 436–450, 2014.

[27] M. Cha, N. B. Alqahtani, X. Yin, T. J. Kneafsey, B. Yao, and Y. Wu, "Laboratory system for studying cryogenic thermal rock fracturing for well stimulation," *Journal of Petroleum Science and Engineering*, vol. 156, pp. 780–789, 2017.

[28] F. H. Li, H. S. Jin, D. H. Hu, B. Wang, and Y. Jia, "Influence of temperature and roughness of surrounding rocks on mechanical behavior of rock bolts," *Soil Dynamics and Earthquake Engineering*, vol. 103, pp. 55–63, 2017.

[29] D. Portnikov and H. Kalman, "The effect of temperature on the mechanical characteristics of individual particles," *Powder Technology*, vol. 336, pp. 393–405, 2018.

[30] A. Nassr, M. Esmaeili-Falak, H. Katebi, and A. Javadi, "A new approach to modeling the behavior of frozen soils," *Engineering Geology*, vol. 246, pp. 82–90, 2018.

[31] A. A. Aleksandrov and M. S. Trakhtengerts, "Viscosity of water at temperatures of -20 to 150 °C," *Journal of Engineering Physics*, vol. 27, no. 4, pp. 1235–1239, 1974.

[32] P. Forst, F. Werner, and A. Delgado, "The viscosity of water at high pressures–especially at subzero degrees centigrade," *Rheologica Acta*, vol. 39, no. 6, pp. 566–573, 2000.

[33] S. Halonen, T. Kangas, M. Haataja, and U. Lassi, "Urea-water-solution properties: density, viscosity, and surface tension in an under-saturated solution," *Emission Control Science and Technology*, vol. 3, no. 2, pp. 161–170, 2017.

[34] A. K. M. B. Alam, Y. Fujii, D. Fukuda, J. Kodama, and K. Kaneko, "Fractured rock permeability as a function of temperature and confining pressure," *Pure and Applied Geophysics*, vol. 172, no. 10, pp. 2871–2889, 2015.

[35] Y. Zhang, Y. S. Zhao, Z. J. Wan, F. Qu, F. K. Dong, and Z. J. Feng, "Experimental study on effect of pore pressure on feldspar fine sandstone permeability under different temperatures," *Chinese Journal of Rock Mechanics and Engineering*, vol. 27, no. 1, pp. 53–58, 2008.